

RSC Advances



This is an *Accepted Manuscript*, which has been through the Royal Society of Chemistry peer review process and has been accepted for publication.

Accepted Manuscripts are published online shortly after acceptance, before technical editing, formatting and proof reading. Using this free service, authors can make their results available to the community, in citable form, before we publish the edited article. This *Accepted Manuscript* will be replaced by the edited, formatted and paginated article as soon as this is available.

You can find more information about *Accepted Manuscripts* in the [Information for Authors](#).

Please note that technical editing may introduce minor changes to the text and/or graphics, which may alter content. The journal's standard [Terms & Conditions](#) and the [Ethical guidelines](#) still apply. In no event shall the Royal Society of Chemistry be held responsible for any errors or omissions in this *Accepted Manuscript* or any consequences arising from the use of any information it contains.



Facile synthesis of well-dispersed CeO₂-CuO_x composite hollow spheres with superior Catalytic Activity for CO oxidation

Jian Zhang^{1,2}, Ming Gong², Yidan Cao², Chang-An Wang^{1*}

Received 00th January 20xx,
Accepted 00th January 20xx

DOI: 10.1039/x0xx00000x

www.rsc.org/

Well-dispersed CeO₂-CuO_x composite hollow spheres have been successfully synthesized through a facile reflux method using carbon spheres as sacrificial templates. The shells of the hollow spheres, ~40 nm in thickness, consist of self-assembled 10-15 nm sized nanoparticles. Scanning electron microscopy (SEM) and Transmission electron microscopy (TEM) were employed to study the structural features of the CeO₂-CuO_x composite hollow spheres. X-ray photoelectron spectrum (XPS) confirmed that most of the copper element distributed on the surface of the CeO₂ shell support. The CeO₂-CuO_x composite hollow spheres exhibited enhanced catalytic activity for CO oxidation: a complete CO conversion could be obtained at 112 °C. The excellent catalytic activity could be ascribed to the hollow structure, high specific surface area and the strong synergistic interaction between CeO₂ and CuO_x.

1. Introduction

Catalytic oxidation of CO has attracted considerable interest over the past several decades due to its potential applications in many fields, including automobile exhausts, fuel cells technology, carbon dioxide lasers and air purification in enclosed atmospheres.^[1-3] Owing to their excellent catalysis activity and low temperature oxidation, precious metal (platinum, gold, palladium, etc.) catalysts are widely studied.^[4-6] However, high prices and low reserves of noble metals have greatly limited their applications in practice. Therefore, more and more researchers have focused on preparation of “noble metal-free” catalysts. Recent studies^[7] reported that a ceria-based transition metal oxide catalyst exhibited enhanced CO oxidation activity due to the synergistic effect between transition metal oxides and ceria. Theoretical studies showed that the synergistic effect can lengthen or weaken the MO (M=transition metal) bond by sharing oxygen at the interface.

Various kinds of composite oxide systems have been synthesized, including CeO₂-CuO_x,^[8,9] CeO₂-ZnCo₂O₄,^[10] CeO₂-MnO₂,^[11] CeO₂-ZnO,^[12] and CeO₂-Fe₂O₃.^[13] Among them, the Ce-Cu binary oxide has

attracted much attention because of its superior catalytic performance towards CO oxidation over other systems. Due to the significant advantages of low cost and high activity, CeO₂-CuO_x catalysts are the most promising “noble

metal-free catalysts” in the future. Most of the traditional methods to synthesize Ce-Cu composite oxides were based on co-precipitation, sol-gel or combustion processes. Although these methods are simple and convenient, the resulting products tend to be unordered and could agglomerate easily in the process of catalytic reactions^[4, 14-16], which seriously aggravates the catalytic activity. Therefore, preparing the Ce-Cu composite oxide highly ordered and well-dispersed is an effective way to improve its performance and durability. For instance, Huizhi Bao et al.^[17] successfully synthesized CeO₂@Cu₂O cubic- and octahedral-structured particles through liquid-solid interfacial reactions using Cu₂O as a sacrificial template. The CeO₂@Cu₂O catalyst showed excellent activity which can attain 100% CO conversion at 170 °C. Dengsong Zhang et al.^[18] demonstrated the preparation of Cu doped CeO₂ nanospheres using a solvothermal method, and 100% CO conversion was obtained at 210 °C. However, it still remains a great challenge for us to further improve the catalytic activity of Ce-Cu catalysts.

Among various nanomaterials, hollow sphere structures have attracted a great deal of attention because of their low density, high porosity and high specific surface area^[19-21]. It is well-known that porosity and specific surface area are important factors concerning catalyst activity. Therefore, over the past few years, many researchers have devoted themselves to developing various techniques to synthesize hollow spheres.^[22] Among all the preparation methods, the template-assisted method is the simplest and most widely used technique. In the process of preparation, the metal oxide nucleates and grows in situ on the surface of the template, which acts as the scaffold for the product, and thus the resulting product inherits the size and morphology of the template.^[20] However, to the best of our knowledge, very few

^a Address here.

^b Address here.

^c Address here.

† Footnotes relating to the title and/or authors should appear here.

Electronic Supplementary Information (ESI) available: [details of any supplementary information available should be included here]. See DOI: 10.1039/x0xx00000x

works have been successful in synthesizing hierarchically well-dispersed CeO₂-CuO_x composite hollow spheres.

In this article, we report a novel self-assembled approach to prepare CeO₂-CuO_x composite hollow spheres in a reflux process, using colloid carbon spheres as sacrificial templates. The obtained CeO₂-CuO_x composite hollow spheres exhibit excellent catalytic activity for CO oxidation.

2. Experimental

Materials:

Cerium(III) nitrate hexahydrate (Ce(NO₃)₃•6H₂O), copper(II) nitrate hydrate (Cu(NO₃)₂•3H₂O), glucose (C₆H₁₂O₆), hexamethyl tetramine (HMT) and absolute ethyl alcohol were used as starting materials. All the reagents are analytically pure and used without further purification. The deionized water used was purified by a Millipore Ultrapure water system.

Processing:

Synthesis of colloid carbon spheres (CSs) templates: In a typical synthesis process, 18g glucose was dissolved in 180ml deionized water to form a clear solution, which was placed in 200ml stainless sealed autoclave and maintained at 180°C for 9 h. A dark brown product was extracted by suction filtration and cleaned by rinsing with deionized water and absolute ethyl alcohol three times, respectively. After dried at 70°C for 12h, the CSs were obtained.

Synthesis of CeO₂-CuO_x composite hollow spheres with different contents (4, 7, 10 and 13mol%): 0.15g CSs was dispersed in 40ml absolute ethyl alcohol through 30min sonicating to form a homogeneous slurry. The 40ml mixed solution, composed of 0.25g HMT and a required amount of Ce(NO₃)₃•6H₂O, Cu(NO₃)₂•3H₂O, was added into the CSs slurry and stirred at room temperature for 2h, followed by reflux at 75°C for 4h before being cooled to room temperature. The CeO₂-CuO_x composite hollow sphere precursor was then filtered and washed with deionized water three times and dried at 80°C for 12h. Finally, a sample of well-dispersed CeO₂-CuO_x composite hollow spheres was completed by heating the precursor at 550°C for 2h in air.

Characterization: The phases of the as-prepared samples were analysed on a Bruker D8-Advance diffractometer using Ni-filtered Cu K α radiation. The working current and voltage was 40 mA and 40 kV, respectively. During the analysis, the samples were scanned from 10° to 90° at 6° /min. S-4800 scanning electron microscope equipped with an EDS and JEOL JEM-1010/2010 transmission electron microscope operated at 200 kV were used to characterize the morphology and microstructure of the samples. The Fourier-transform infrared (FT-IR) spectra for each sample were measured by a Nicolet Magna 750. Thermogravimetric (TG-DSC) analyses were performed on a SDT Q600(TA-Instruments). A NOVA 4000 automated gas sorption system was used to ascertain the BET-surface area. X-ray photoelectron spectra were taken to

investigate the surface valence states of Ce and Cu species in each composite hollow sphere sample.

CO oxidation: The catalytic activity test was carried out in a fixed-bed flow micro-reactor at atmospheric pressure. In a typical experiment, 100mg of the as-prepared sample was added into the micro-reactor. The sample was pre-treated at 350°C for 1h in air, followed by purging with highly pure N₂ gas for 15 min. After the cooling process in the microreactor, a gas mixture of CO/O₂/N₂(0.8:20:79.2) was passed through the reactor. Real-time concentrations of CO and CO₂ of the resulting gases were analysed using an infrared gas analyser. The CeO₂ hollow spheres and CeO₂ particles were also tested for a better comparison.

Results and discussion

The CeO₂-CuO_x composite hollow spheres were prepared by employing carbon sphere as hard template. The as-prepared carbon spheres were monodispersed with a rather smooth surface, and the average diameter of the carbon spheres is about 400nm (supplementary figure1). Yadong Li et al.^[23] reported that carbon spheres had a large number of organic functional groups including -COOH, -CHO, and -OH on their surface, which is an indispensable qualification for coating. Owing to the negative charge of carbon spheres, certain metal ions can be adsorbed on their surface. With the help of a precipitant (HMT), the adsorbed metal ions will nucleate and turn into a nanooxide precipitate under reflux. After the process of self-assembly, uniform composite oxide shells can be achieved. Figure 1a shows SEM images of CS/CeO₂-CuO_x microspheres, which indicate that all of the particles were still monodispersed and inherited the morphology of the carbon sphere templates. No uncoated particles were found. A magnified image (the inset of Figure 1a) shows the detail of the rough surface of these microspheres, which can be attributed to the layer by layer self-assembly of grain. Additionally, the rough surface reveals the presence of a complete and homogenous shell on the carbon sphere template, which was further verified by the TEM images of the CS/CeO₂-CuO_x composite microsphere (figure 1b). The interface between the core and shell can be clearly observed and the thickness of the shell is about 40nm. It is worth to mention that the thickness of the shell can be easily tuned by adjusting the concentration of the corresponding metal salts at the beginning of the reaction. Figure 1c shows the SEM images of CeO₂-CuO_x composite hollow spheres obtained after the thermal treatment. The majority of obtained spheres were homogenous in size and spherical in shape, and only very few are broken down. The magnified micrographs (the inset of Figure 1c) show that the surface of the microspheres was coarse, which is characteristic of mesoporous materials. Several spheres cracked (as the red arrows point out), demonstrating that the microspheres are hollow structures, which is further confirmed by TEM images (Figure 1d). Moreover, the diameter of composite microspheres was found to decrease from 480nm to 400nm after calcination. This can be attributed to the sintering contraction of nanoparticles and

further condensation of molecular precursors upon calcinations^[24]. Figure 1d displays a TEM image of CeO₂-CuO_x composite hollow spheres where intact shells composed of nanoparticles can be clearly observed which correspond to the results of SEM. In addition, it can be observed the shell possess a porous structure with a macro-pore located at the center of nano-sphere. This hierarchical structural characteristic endows the sample with a high porosity and specific surface area. From the magnified TEM images (Figure 1e), it is clear that the shell was made up of numerous particles with particle sizes ranging from 10 nm to 15 nm. The lattice fringes in the high-resolution TEM (Figure 1f) image show a spacing approximately 0.31 nm corresponding to the (111) planes of face-centered cubic fluorite structured CeO₂. The corresponding SAED patterns (supplementary figure 2) suggest a single presence of CeO₂ diffraction rings. Although the results seem strange, similar results were also reported in other references^[25].

Figure 1. SEM and TEM images of (a) (b) CS@CeO₂-CuO_x, the inset manifests magnified micrograph; (c) (d) CeO₂-CuO_x composite hollow sphere, red arrow points out the cracked hollow sphere. (e) (f) high-resolution TEM images of CeO₂-CuO_x hollow sphere.

In order to confirm the presence of both Ce species and Cu species in the shell of the composite microsphere, an energy dispersive spectroscopy (EDS) mapping analysis of the sample was conducted. The results are shown in Figure 2b to Figure 2e, where the yellow, red, green and pink regions refer to the elements of Ce, Cu, C and O, respectively. The results confirmed that both Ce and Cu species exist in the shell of the hollow spheres. The size of the C-enriched area was smaller than that of the area enriched in other elements, which indicated that there was a uniform coating layer on the surface of the carbon sphere. However, it should be mentioned that the copper species content was only 10 mol%, but from the spectroscopy, the content of Cu species seemed to be higher than that of Ce species, and there were two possible explanations for this phenomenon. Firstly, the TEM sample holder is made of copper, so it could influence the results. Secondly, the Cu species tend to be concentrated on the surface of the composite hollow sphere owing to its lower specific surface energy than that of the Ce species. The EDS patterns (Figure 2f) also revealed that the composite hollow spheres contained both Ce and Cu species and that the mole ratio of Ce/Cu was 8.97/2.65.

Figure 2. TEM (a) and element mapping (b, c, d, e) images of CeO₂-CuO_x@CS composite microsphere, and EDS energy spectrum of CeO₂-CuO_x hollow sphere (f).

To investigate the phase composition of the samples, X-ray powder diffraction was performed and the results are shown in Figure 3a. All the diffraction peaks can be indexed to the cubic fluorite structured CeO₂ crystal (JCPDS 34-0394), which is in good agreement with the results of SAED and HRTEM. The broad nature of the patterns indicated that the CeO₂-CuO_x composite hollow spheres were composed of nanocrystals, which is consistent with the results of TEM analysis. No peak can be indexed to copper species. This can possibly be explained by the findings of previous researchers, who reported that the copper species cannot be detected by XRD when the contents is below 20 mol%^[25].

X-ray photoelectron spectroscopy was conducted to determine the valence states of Ce and Cu in the composite hollow sphere, and the results are shown in Figure 3c and d, respectively. Six significant peaks (916.52, 907.22, 900.57, 898.02, 888.62 and 882.27 eV) clearly exist in the Ce 3d spectra, and they are all attributed to Ce(IV) feature. In the

Cu2p spectrum, both Cu₂O (Cu2p_{3/2} binding energy around 932.5eV) and CuO (Cu2p_{3/2} binding energy around 933.7 eV) features were observed^[17]. The Cu/Ce atomic ratio in the surface of the CeO₂-CuO_x composite hollow spheres were detected by XPS and displayed in Table1. For CeO₂-CuO_x composite hollow spheres, the Cu/Ce atomic ratio on the surface is always higher than that of the real Cu/Ce molar ratio. It increases almost linearly with the corresponding real Cu/Ce mole ratio. Therefore, it can be concluded that the Cu species are highly concentrated on the surface of CeO₂ hollow spheres. The Raman spectra of the samples prepared with various amounts of copper species are illustrated in Figure3b. The peak centered at 461cm⁻¹ is assigned to the symmetric breathing mode of oxygen atoms around cerium ions in the fluorite cerium oxide phase. It can be observed that with the increase of concentration of Cu species, the intensity of the peak decreases and the peak position shifts towards the low wavenumber area because of the strong interaction between the copper species and the CeO₂ shell. It is worth to mention that the interaction between CeO₂ and copper species can be divided into two aspects. As mentioned above (XPS spectra), copper species highly dispersed on the surface of CeO₂ shell. The interaction between copper species and CeO₂ contributes to the weakening of the metal-Oxygen bond by sharing oxygen at the interface, which were the active sites for CO Oxidation^[9]. Moreover, there are small number of copper species incorporates into the CeO₂ lattice replace Ce⁴⁺. Due to the copper ion radius (0.072nm) is smaller than that of Ce⁴⁺ (0.097nm), So the Raman band shifts to low wavenumber with the increase of copper species.

Figure3 XRD pattern of the composite CeO₂-CuO_x hollow sphere(a), Raman spectra of the as-prepared composite CeO₂-CuO_x hollow sphere and pure CeO₂ hollow sphere(b), XPS spectra of Ce3d of the composite CeO₂-CuO_x hollow sphere(c) and Cu2p of the composite CeO₂-CuO_x hollow sphere (d).

The FT-IR spectra of CS, CS/CeO₂-CuO_x composite microspheres, CeO₂-CuO_x (550°C heat-treated) hollow spheres

are show in Figure4a. The bands centered around 3462, 1706 and 1618cm⁻¹ correspond to -OH, C=O and C=C vibrations, respectively. In addition, the bands in the range of 1000-1300cm⁻¹ contain C-OH stretching and OH bending vibrations^[21]. All of these functional groups can be attributed to the CS templates. It is interesting that after the coating of CeO₂-CuO_x composite precursor, the intensity of all these peaks did not decrease, but instead increase. This strange phenomenon can be explained as follows: The surface of the original carbon sphere template is hydrophilic, and Sa Lietai^[22] reported that alkaline environment can help to increase the content of oxygen-containing groups, rendering the surface of the CS more hydrophilic. As the precipitant HMT provided an alkaline environment, the intensity of the feature peaks increased. After the thermal treatment at 550°C, all the characteristic peaks of CS almost disappeared, signifying the complete removal of the template from the composite oxide.

Thermogravimetric (TG-DSC) analysis was employed to further investigate the CS/CeO₂-CuO_x composite particles (Figure4b). The weight loss can be divided into two stages. The first one occurs within a temperature range of 100 to 250°C, about 5wt%, which results from the removal of absorbed water and the residual solvent of composite particles. The second one, from 250 to 380°C, is a significant weight loss of ~55wt%, which can be attributed to the decomposition and oxidation of the carbon sphere. Finally, 40wt% CeO₂-CuO_x composite hollow spheres can be achieved from CS/CeO₂-CuO_x.

Figure.4(a) FT-IR spectra of CS, CS/CeO₂-CuO_x nanospheres, CeO₂-CuO_x (550°C heat-treated) and CeO₂-CuO_x (750°C heat-treated) composite hollow spheres (b) TG-DSC results of CS/CeO₂-CuO_x nanospheres.

CO catalytic oxidation tests were conducted to investigate the catalytic activity of the CeO₂-CuO_x composite hollow spheres. Pure CeO₂ hollow spheres and CeO₂ nanoparticles were prepared and acted as control catalysts. T50, the temperature for 50% CO conversion is used to estimate the catalytic activity of the sample. The catalytic results for the above samples are shown in Figure5. As can be seen, the catalytic activity of the samples following such order of T50: 10%CuO_x-CeO₂ > 13%CuO_x-CeO₂ > 7%CuO_x-CeO₂ > 4%CuO_x-CeO₂ > CeO₂ hollow sphere > CeO₂ particle, and corresponding T50 values shown in table1. Furthermore, the T90 values of all CuO_x-CeO₂ composite hollow spheres are under 150°C. For the samples D, E and F, the complete CO conversions attained at 112, 127 and 130°C, respectively. While the light-off temperature of pure CeO₂ hollow spheres and CeO₂ nanoparticles reached as high as 150°C, 90% CO conversion was obtained at 272 and 286°C,

respectively. Obviously, the CeO₂-CuO_x composite hollow spheres possess much higher catalytic activity than pure CeO₂ hollow spheres and CeO₂ nanoparticles. The 10% CuO_x-CeO₂ composite hollow spheres had the highest catalytic activity. The enhanced performance can be attributed to the strong synergistic interaction between copper species and cerium. From the results of XPS and XRD, it can be known that the copper species are well dispersed on the surface of CeO₂, and the two phase interfaces act as chemisorption sites for CO^[9]. It is obviously found that, below 10mol%, the increasing copper species contents can effectively increase the catalytic performance, which can be attributed to the increase of the active sites for CO catalytic oxidation. However, upon further increase of the amount of copper species, the bulk CuO_x will form and can aggravate the catalytic activity^[25]. So in this experiment, the optimal content of copper species was found to be around 10mol%. Next, a cycling test was performed to study the stability of 10%CuO_x-CeO₂ composite hollow spheres (figure6). After five reaction cycles from 30 to 140°C, the sample still maintains high catalytic activity with 100% CO conversion at 125°C, which demonstrate the good cycle stability of CeO₂-CuO_x composite hollow spheres.

Figure.5 CO conversion as a function of temperature for (A) CeO₂ hollow sphere (B)CeO₂ solid particle (C)4%(D)7%(E)10%(F)13% CuO_x-CeO₂ composite hollow spheres.

Figure.6 cycle test of 10%CuO_x-CeO₂ composite hollow spheres

The specific surface area also plays an important role in catalytic oxidation. It is well-known that a high surface area endows catalyst with better catalytic activity, due to the fact that higher surface areas can provide more active sites. The N₂ adsorption-desorption isotherms of CeO₂ and CeO₂-CuO_x composite hollow spheres are illustrated in FigureS3. All the samples exhibited type IV isotherms with H₂ type hysteresis loops, indicating typical mesoporous structures. The specific surface areas of all the samples are summarized in Table 1. As can be seen, the specific surface area of the CeO₂-CuO_x composite hollow spheres will be increased along with the increase of copper species contents at first and then decreased when the content of copper species is more than 10mol%. There is no doubt that copper species are the active sites for CO oxidation, so the increase of specific surface area and copper species means the increase of reactivity sites when the contents of

copper species stay below 10mol%. Therefore, corresponding T50 values decrease. However, the T50 values actually decrease when the content of copper species is more than 10mol%. It is related to the formation of bulk CuO_x as mentioned above, since the activity of bulk CuO_x is lower than highly dispersed CuO_x.^[9]

Table1 the surface Cu mole percentage, (BET) surface area (m²/g) and T50 values of samples

Conclusions

In summary, we developed a simple self-assembly method to prepare CeO₂-CuO_x composite hollow spheres using colloid carbon spheres as sacrificial templates. The hollow structures can be obtained after a simple thermal treatment in an air environment. Copper species are highly dispersed on the surface of CeO₂ shell. Due to the high specific surface area and the strong synergistic interaction between CeO₂ and CuO_x in the CeO₂-CuO_x composite hollow spheres, the samples display excellent catalytic activity for CO oxidation. 10mol% Cu species is the optimal content in the composite oxide, which can attain 100% CO conversion at 112°C. In particular, this method performed admirably and can be easily extended to synthesize other composite hollow spheres.

Acknowledgements

The authors would like to thank the financial support from the National Science Foundation of China (NSFC-No. 51221291 and 51172119).

Notes and references

- 1 D. Gamarra, C. Belver, M. Fernández-García and A. Martínez-Arias, *J. Am. Chem. Soc.*, 2007, 129, 12064-12065.
- 2 P. G. Harrison, I. K. Ball, W. Azelee, W. Daniell and D. Goldfarb, *Chem. Mater.*, 2000, 12, 3715-3725.
- 3 X. Zheng, X. Zhang and Fang, *Catal. Commun.*, 2006, 701-704.
- 4 P. Bera, A. Gayen and M. S. Hegde, *J. Phys. Chem. B.*, 2003, 107, 6122-6130.
- 5 S. Carrettin, P. Concepción, A. Corma, J. M. López Nieto and V. F. Angew. Chem.-Int. Edit., 2004, 43, 2538-2540.
- 6 X. Wang, D. Liu, S. Song and H. Zhang, *J. Am. Chem. Soc.*, 2013, 135, 15864-15872.
- 7 V. Shapovalov and H. Metiu, *J. Catal.*, 2007, 245, 205-214.
- 8 J. Qin, J. Lu, M. Cao and C. Hu, *Nanoscale*, 2010, 2, 2739-2743.
- 9 A. Jia, S. Jiang, J. Lu and M. Luo, *J. Phys. Chem. C.*, 2010, 114, 21605-21610.
- 10 F. Wang, X. Wang, D. Liu, J. Zhen, J. Li, Y. Wang and H. Zhang, *ACS Appl Mater Inter.*, 2014, 6, 22216-22223.

- 11 G. Chen, F. Rosei and D. Ma, *Adv. Funct. Mater.*, 2012, 22, 3914-3920.
- 12 Q. Xie, Y. Zhao, H. Guo, A. Lu, X. Zhang, L. Wang, M. Chen and D. Peng, *ACS Appl. Mater. Inter.*, 2013, 6, 421-428.
- 13 G. Avgouropoulos and T. Ioannides, *Catal Lett.*, 2007, 116, 15-22.
- 14 R. Prasad and G. Rattan, *Bulletin of Chemical Reaction Engineering & Catalysis*, 2010, 5, 7-30.
- 15 Lopez. Camara, Antonio, Kubacka. Anna and Schay. Zoltan, *J Power Sources*, 2011, 9, 4364-4369.
- 16 S. H. Zeng, Y. Liu and Y. Q. Wang, *Catal. Lett.*, 2007, 117, 119-125.
- 17 H. Bao, Z. Zhang, Q. Hua and W. Huang, *Langmuir*, 2014, 30, 6427-6436
- 18 D. Zhang, Y. Qian, L. Shi, H. Mai, R. Gao, J. Zhang, W. Yu and W. Cao, *Catal Commun*, 2012, 26, 164-168.
- 19 J. Wang, N. Yang and Tang, *Angew. Chem.-Int. Edit.*, 2013, 6545-6548.
- 20 M. Agrawal, S. Gupta, A. Pich, N. E. Zafeiropoulos and M. Stamm, *Chem Mater*, 2009, 21, 5343-5348
- 21 M. Chen, C. Ye, S. Zhou and L. Wu, *Adv. Mater.*, 2013, 25, 5343-5351.
- 22 C. Wang, S. Li and L. An, *Chem. Commun*, 2013, 49, 7427-7429.
- 23 X. Sun and Y. Li, *Angew. Chem.-Int. Edit.*, 2004, 43, 597-601.
- 24 D. Wang and F. Caruso, *Chem Mater*, 2002, 14, 1909-1913.
- 25 M. Luo, Y. Song, J. Lu, X. Wang and Z. Pu, *J. Phys. Chem. B.*, 2007, 111, 12686-12692.

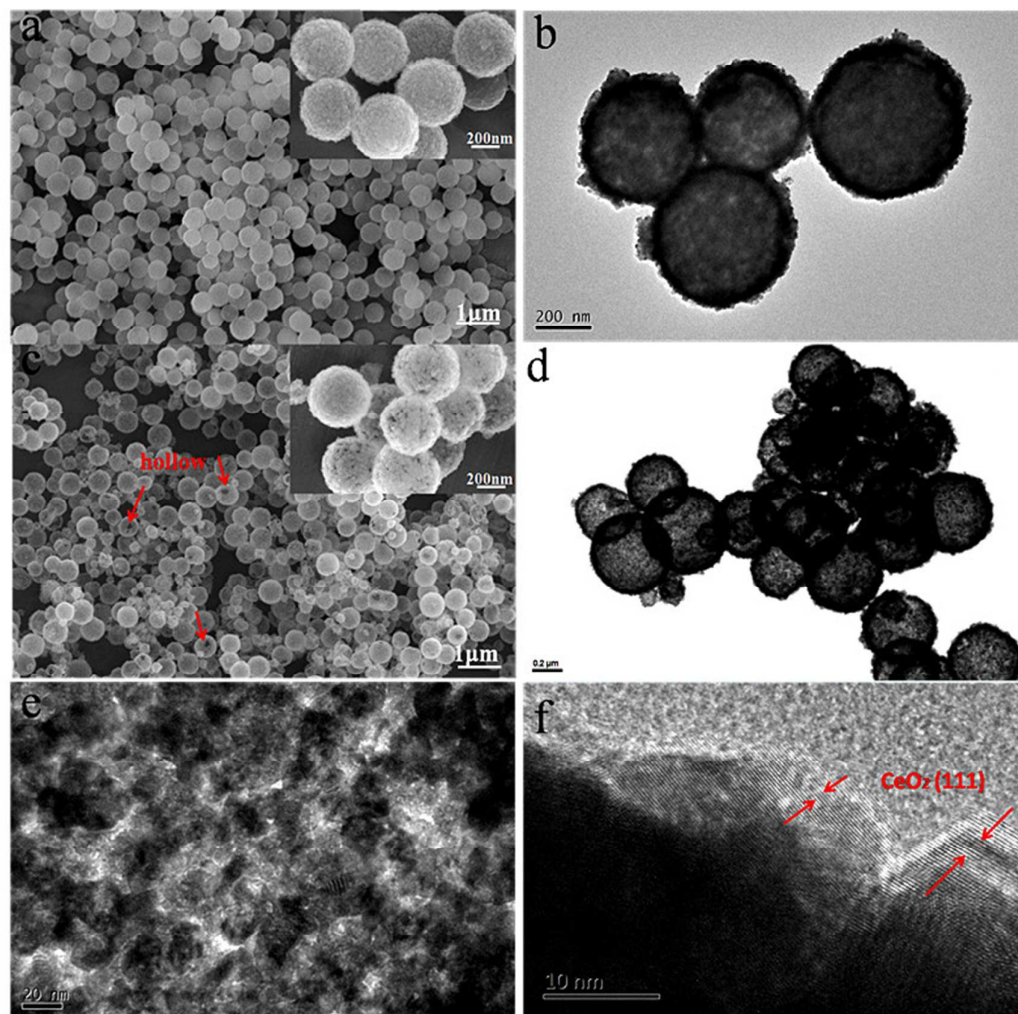


Figure 1. SEM and TEM images of (a)(b)CS@CeO₂-CuOx, the inset manifests magnified micrograph; (c)(d)CeO₂-CuOx composite hollow sphere, red arrow point out the cracked hollow sphere. (e)(f)high-resolution TEM images of CeO₂-CuOx hollow sphere.

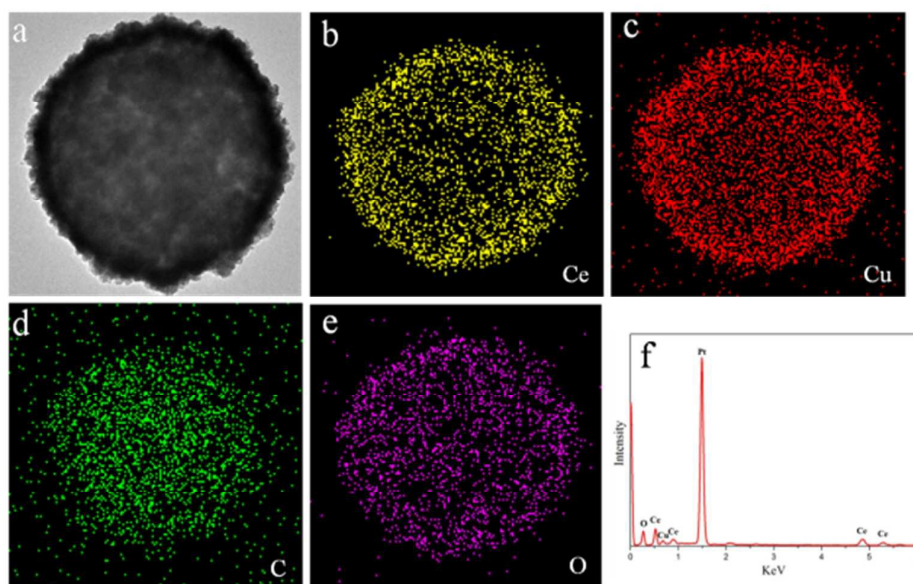


Figure 2. TEM (a) and element mapping (b, c, d, e) images of CeO₂-CuO_x@CS composite microspheres, and EDS energy spectrum of CeO₂-CuO_x hollow sphere (f).

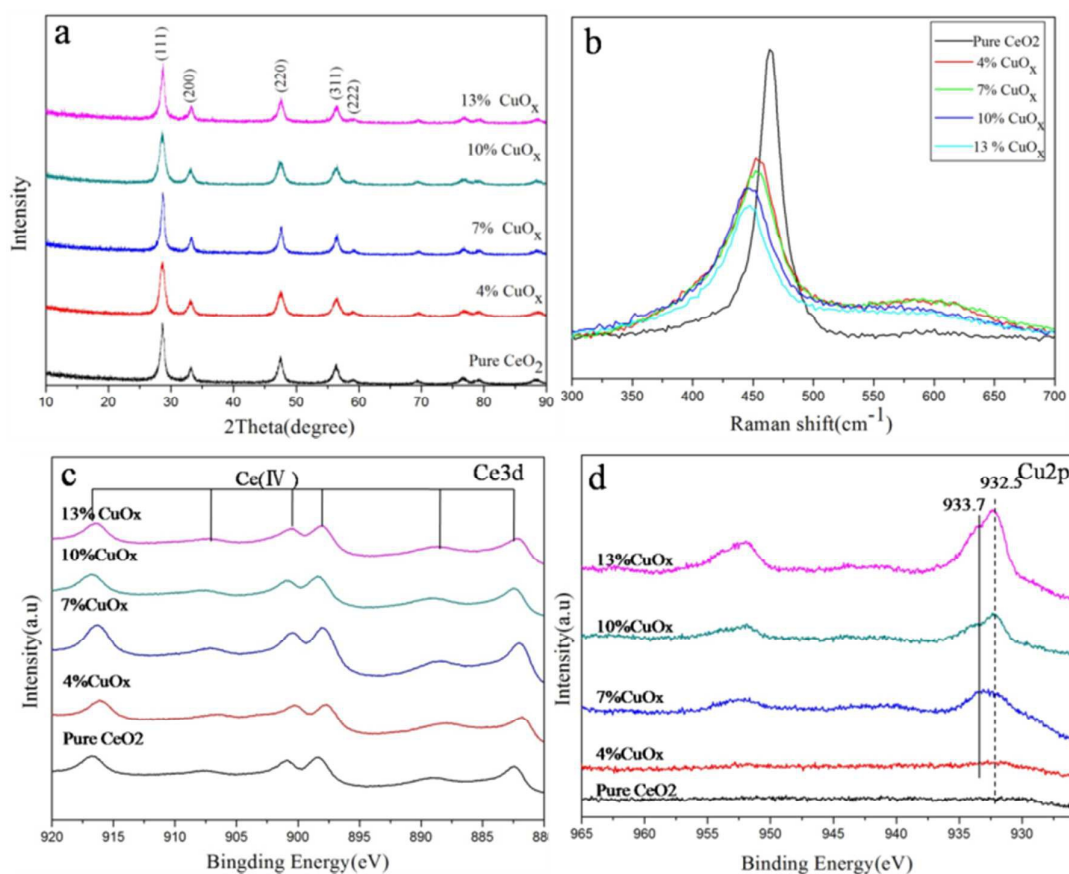


Figure 3. XRD pattern of the composite CeO₂-CuO_x hollow sphere (a), Raman spectra of the as-prepared composite CeO₂-CuO_x hollow sphere and pure CeO₂ hollow sphere (b), XPS spectra of Ce 3d of the composite CeO₂-CuO_x hollow sphere (c) and Cu 2p of the composite CeO₂-CuO_x hollow sphere (d).

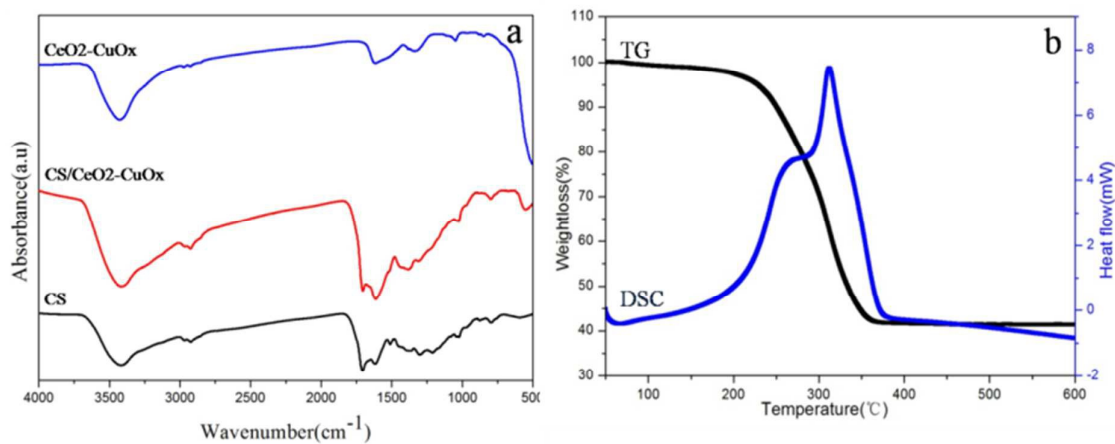


Figure.4(a)FT-IR spectra of CS, $\text{CS/CeO}_2\text{-CuO}_x$ nanospheres, $\text{CeO}_2\text{-CuO}_x$ (550 $^\circ\text{C}$ heat-treated) and $\text{CeO}_2\text{-CuO}_x$ (750 $^\circ\text{C}$ heat-treated) composite hollow spheres(b)TG-DSC results of $\text{CS/CeO}_2\text{-CuO}_x$ nanospheres.

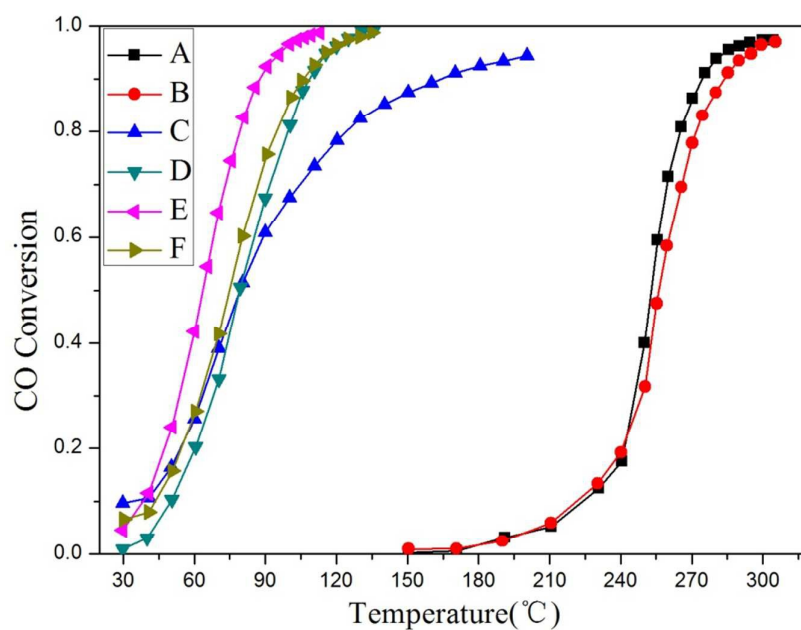


Figure.5 CO conversion as a function of temperature for (A) CeO_2 hollow sphere (B) CeO_2 solid particle (C)4%(D)7%(E)10%(F)13% $\text{CuO}_x\text{-CeO}_2$ composite hollow sphere

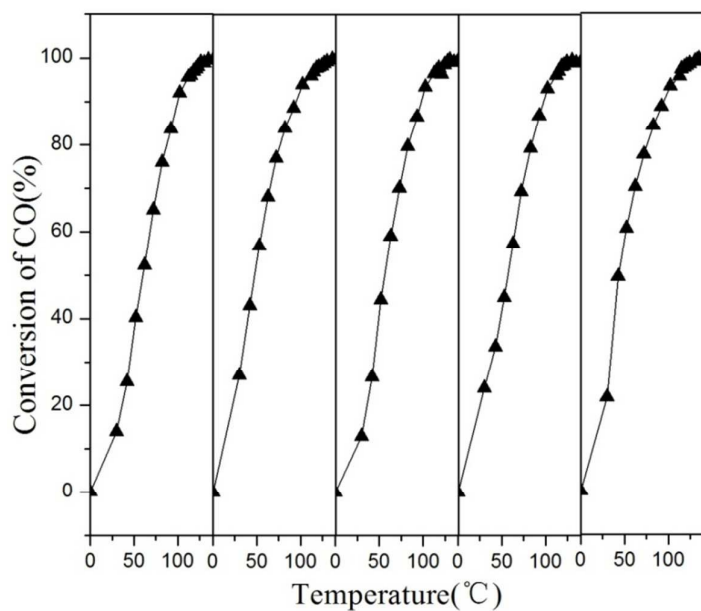


Figure6.Cycle test of 10%CuO_x-CeO₂ composite hollow spheres

Table.1. the surface Cu mole percentage, (BET) surface area (m²/g) and T₅₀ values of the samples

sample	Pure CeO ₂	4%CuO _x -CeO	7%CuO _x -CeO	10%CuO _x -CeO	13%CuO _x -CeO
		2	2	2	2
Surface Cu mole percentage	0	16.5%	22.7%	28.3%	28.7%
(BET)Surface area(m ² /g)	87.23	98.72	118.62	123.67	105.85
T ₅₀ (Temperature for 50% CO conversion)	253°C	82°C	79°C	65°C	74°C